

ROLE OF FLUCTUATIONAL ELECTRODYNAMICS IN NEAR-FIELD RADIATIVE HEAT TRANSFER

Mathieu Francoeur and M. Pinar Mengüç
Radiative Transfer Laboratory, Department of Mechanical Engineering
University of Kentucky, Lexington, KY 40506-0503, USA
www.engr.uky.edu/rtl

ABSTRACT. The objective of this paper is to discuss the role of fluctuational electrodynamics in the context of a generalized radiative heat transfer problem. Near-field effects, including the interference phenomenon and radiation tunneling, are important for applications to nanostructures. The classical theory of radiative transfer cannot be readily applied as the feature size approaches the dominant wavelength of radiative emission. At all length scales, however, propagation of radiative energy is properly represented by electromagnetic wave approach, which requires the solution of the Maxwell equations. The fluctuational electrodynamics provides a model for thermal emission when solving a near-field radiation heat transfer problem, and the fluctuation-dissipation theorem provides the bridge between the strength of the fluctuations of the charges inside a body and its local temperature. This paper provides a complete and systematic derivation of the near-field radiative heat flux starting from the Maxwell equations. An illustrative example of near-field versus far-field radiation heat transfer is presented, and the length scale for transition from near- to far-field regime is discussed; the preliminary results show that this length scale can be as large as three times than predicted from Wien's law.

NOMENCLATURE

A	magnetic vector potential, Wb m ⁻³	k	wavevector, rad m ⁻¹	Φ_e	electric scalar potential, V
B	magnetic flux density vector, Wb m ⁻²	n	index of refraction, $n'+in''$	μ	magnetic permeability, N A ⁻²
D	electric flux density vector, C m ⁻²	$r_{ij}^{s,p}$	Fresnel's reflection coefficients	Θ	mean energy of a Planck oscillator, J
d	gap thickness, m	r	position vector, m	ρ_e	electric charge density, C m ⁻³
E	electric field vector, V m ⁻¹	S	Poynting vector, W m ⁻²	σ	electric conductivity, C ² N ⁻¹ m ⁻¹ s ⁻¹
F	generalized force, N	\dot{V}	generalized velocity, m s ⁻¹	Subscripts and superscripts	
g	Green's function, m ⁻¹	Z	impedance matrix, Ω	0	refers to vacuum
$\overset{e,m}{\mathbf{G}}$	electric/magnetic dyadic Green's function, m ⁻¹	Greek symbols		*	complex conjugate
H	magnetic field vector, A m ⁻¹	δ	Dirac function	', ''	source point
i	complex constant, (-1) ^{1/2}	ϵ	complex electric permittivity, C ² N ⁻¹ m ⁻²	r	random variable
\mathbf{I}	idem factor	$\hat{\epsilon}$	electric permittivity, C ² N ⁻¹ m ⁻²	s, p	polarization states
J	current density vector, A m ⁻²	ϵ_r	dielectric constant, $\epsilon_r' + i\epsilon_r''$	<i>evan</i>	evanescent modes
				<i>prop</i>	propagating modes

INTRODUCTION

With the recent advances in nanotechnologies, there is strong motivation for diagnostics and material processing with nanometer resolution. This necessitates understanding and application of precision controlled energy and heat transfer mechanisms for the development of novel engineering platforms. At the nanometer scale, traditional heat transfer formulations for conduction and

radiation cease to be valid. For example, the Fourier conduction law starts deviating from its familiar form once the length scales fall below about 20 nm, depending on the material properties [1]. Proper analysis of diffusion heat transport at such small regime requires consideration of energy carriers responsible for heat conduction, namely electrons, atoms, molecules, and phonons (lattice vibrations) [2]. While heat conduction at nanoscale has been studied extensively over the past few years, the heat transfer community has paid relatively little attention to radiation heat transfer in nanostructures.

It is quite known that theoretical predictions of radiative heat transfer between closely spaced bodies can exceed the values predicted by the Planck blackbody distribution by several orders of magnitude [3-5]. This deviation from the classical theory is due to the so-called near-field effects. In this paper, we use “near-field radiative heat transfer” to describe underlying physics rather than the adjective “nanoscale.” Radiative heat transport in nanostructures always involves near-field effects. Yet, near-field effects may also have significant contributions in structures larger than nanosizes; for example, in cryogenic applications [4,5].

Near-field contribution of radiative energy can be accounted for in calculations if the electromagnetic waves are considered as the mechanism for energy propagation and the Maxwell equations are solved with the proper boundary conditions. The importance of the Maxwell equations on radiative transfer is thoroughly discussed by Mishchenko [6,7]. For prediction of thermal emission, the fluctuational electrodynamics need to be used, leading to the stochastic Maxwell equations [8]. The main objective of this paper is to clearly outline the role of fluctuational electrodynamics in the context of a generalized radiation heat transfer problem. In the same manner, this work also aims to provide a comprehensive discussion of the far-field and near-field regimes, by defining the models and approximations used for each case. The last objective is to provide a systematic and relatively simple derivation of the mathematical model used for near-field calculations.

The next section is devoted to an overview of the fundamental processes of radiation heat transfer and associated models. Subsequently, the derivation of a general expression for the radiative flux in the near-field is provided starting from the Maxwell equations and using the fluctuational electrodynamics. An example of near-field versus far-field predictions is presented, and the length scale for transition between these two regimes is discussed. Finally, the last section is devoted to a summary of the discussion.

FUNDAMENTAL PROCESSES IN RADIATIVE HEAT TRANSFER

Radiative heat transfer can be categorized in terms of four fundamental processes: emission, absorption, scattering, and propagation of radiative energy. In general terms, emission refers to *how* the radiative energy emanates from an object, where its internal energy is converted to propagating electromagnetic waves. Absorption is when these waves interact with a body and the energy is converted back into the internal energy of the object. Scattering is defined as the re-direction of radiant energy, and involves the phenomena of refraction, reflection, transmission, and diffraction.

If the size between objects exchanging radiant energy is much larger than the dominant wavelength of radiation, the radiative energy propagation is considerably simplified by using ray tracing or geometric optics approximations. This approach implies that the energies of two rays incident at a given point are simply added without any consideration of their respective phases. The classical theory of radiation heat transfer is based on this simplification, which is necessary for calculation of radiative exchanges between large number of surfaces and volume elements separated by participating gases and particles. The radiative transfer equation (RTE) describes the conservation of intensity along a line of sight at a given wavelength [9,10]. The emission of thermal radiation is included in the RTE via the Planck law. Derivation of the Planck blackbody radiation formulation, which is based on the statistical mechanics approach of Boltzmann, is widely credited for opening

the path towards quantum mechanics. In the classical sense, attenuation (absorption and out-scattering) along the line-of-sight are linearly related to the radiative intensity, where the proportionality constants are called the absorption coefficient (m^{-1}) and the scattering coefficient (m^{-1}), respectively. For the in-scattering term, the probability that a ray coming from any direction being scattered in the direction for which the RTE is solved is given by the scattering phase function. These proportionality constants can be derived from quantum mechanical information, but also by following the wave theory [7]. For example, when dealing with particulate media, it is necessary to use the electromagnetic wave approach to calculate the scattering and absorption cross-sections and coefficients, as well as the scattering phase function. Radiative properties of ideal surfaces can also be theoretically predicted using the electromagnetic wave approach, provided the fundamental properties, i.e., spectral electric permittivity and magnetic permeability, are available.

In the most strict sense, emission of thermal radiation from a body at finite temperature can be explained by quantum mechanics. A body loses energy due to emission, which is as a result of an electron bounding an atom falling to a lower energy level. This emitted energy is associated with the concept of “photons,” which has been questioned for some time (see Kidd [11] and Mischenko [6] and references there in). As shown in [6,7], electromagnetic wave approach is physically more accurate to represent the propagation of radiative energy. Absorption, which is also explained by quantum mechanics, occurs when the wave incident on an atom or molecule has sufficient and necessary energy to raise the energy of one of electrons to a higher energy level. The scattering processes are also fundamentally due to quantum effects. If the energy of radiation incident on an atom is too small to cause a transition to a higher energy level, there is no atomic transition. Nevertheless, the cloud of electrons bounding the atom starts vibrating at the frequency of the incident light. This system constitutes an oscillating dipole (with respect to the positive nucleus) and instantaneously begins to radiate at the same frequency. The resulting scattered radiation consists of a radiation propagating in some random direction. If the scattered radiation carries the same amount of energy as the incident radiation, then scattering is considered as elastic. Yet, sometimes scattering by an atom or molecule occurs at a frequency different than the original energy (or frequency, as the wave energy is related to its frequency via $\hbar\omega$). This is called inelastic scattering. However, these quantum mechanics descriptions cannot be readily used in solving radiative heat transfer problems in most practical applications. Instead, simplified models are used to model the emission, absorption, and scattering processes as described above when the RTE is to be solved.

When two bodies exchanging thermal radiation are spaced by a distance of the same order of magnitude as the dominant emission wavelength, the near-field effects come into picture. Traditionally, this critical wavelength is determined from the Wien law, and corresponds to the wavelength of the peak emission according to the Planck blackbody distribution. Near-field effects which affect radiative exchange significantly are the interference phenomenon and radiation tunneling, which includes the resonant excitation of surface polaritons (plasmons and phonons). Since the wave nature of thermal radiation is neglected when solving the RTE, the near-field effects are not accounted for. To circumvent this problem, radiative transfer between closely spaced bodies should be analyzed starting from the Maxwell equations, by considering the propagation of energy as electromagnetic waves. The phenomenon of absorption of electromagnetic waves in that case is included in the dielectric constant of the material. The scattered field can be calculated directly via the Maxwell equations by assuming that the total field is the superposition of an incident and scattered field. A mathematical model to describe the emission process is needed, and is provided by the fluctuational electrodynamics, which is discussed in the next section.

NEAR-FIELD RADIATIVE HEAT TRANSFER

Stochastic Maxwell equations and fluctuational electrodynamics From an electromagnetic point of view, the emission of thermal radiation can be described as follows. If an object is at temperature T greater than 0 K, thermal agitation causes a chaotic motion of charged particles inside the body. These charged particles are electrons in metals and ions in polar crystals. The random fluctuations of the charges generate in turn a fluctuating electromagnetic field, called thermal radiation field (as it originates from random thermal motion) [12]. On a macroscopic level, the field fluctuations are due to thermal fluctuations of the volume densities of the charges and current. In other words, the electromagnetic field generated thermally is *not* the sum of the fields of the individual charges, but is a field produced by sources that are also macroscopic (volume densities of charge and current). The fluctuational electrodynamics (FE) is built on this simple macroscopic description. Since it is based on fluctuations around an equilibrium temperature T , the theory is thus applicable to media of any forms in local thermodynamic equilibrium, where an equilibrium temperature can be defined in any given point inside the body at any instant [13]. The FE approach is at some point also applicable to non-equilibrium conditions, in cases where the transport phenomena required to maintain steady-state conditions are negligible when compared with the energy emitted by the body [8,13]. The FE is the key for solving near-field radiation heat transfer problems, since it allows calculation of thermal emission starting from the Maxwell equations, which otherwise describe only the propagation of electromagnetic waves.

The Maxwell equations are expressed as (we assume throughout this paper that the materials are non-magnetic) [14,15]:

$$\nabla \times \mathbf{E}(\mathbf{r}, \omega) = i\omega \mathbf{B}(\mathbf{r}, \omega) = i\omega \mu_0 \mathbf{H}(\mathbf{r}, \omega) \quad (\text{Faraday's law}) \quad (1a)$$

$$\begin{aligned} \nabla \times \mathbf{H}(\mathbf{r}, \omega) &= -i\omega \mathbf{D}(\mathbf{r}, \omega) + \mathbf{J}(\mathbf{r}, \omega) = -i\omega \hat{\epsilon} \mathbf{E}(\mathbf{r}, \omega) + \sigma \mathbf{E}(\mathbf{r}, \omega) = -i\omega (\hat{\epsilon} + i\sigma/\omega) \mathbf{E} \\ &= -i\omega \epsilon \mathbf{E}(\mathbf{r}, \omega) \quad (\text{Ampère's law}) \end{aligned} \quad (1b)$$

$$\nabla \cdot \mathbf{D}(\mathbf{r}, \omega) = \nabla \cdot (\hat{\epsilon} \mathbf{E}(\mathbf{r}, \omega)) = \rho_e \quad (\text{Gauss's law}) \quad (1c)$$

$$\nabla \cdot \mathbf{B}(\mathbf{r}, \omega) = \nabla \cdot (\mu_0 \mathbf{H}(\mathbf{r}, \omega)) = 0 \quad (\text{Gauss's law}) \quad (1d)$$

with the continuity equation:

$$\nabla \cdot \mathbf{J}(\mathbf{r}, \omega) = i\omega \rho_e \quad (2)$$

where it has been assumed that the time-harmonic fields have the form $\exp(-i\omega t)$. In Ampère's law, $\hat{\epsilon}$ is the electric permittivity of the material (real number). The combination of the electric permittivity and electric conductivity ($\hat{\epsilon} + i\sigma/\omega$) leads to a complex electric permittivity, denoted by ϵ . The dielectric constant ϵ_r of the material is then defined as the ratio of the complex electric permittivity ϵ and the electric permittivity of the vacuum ϵ_0 .

From the qualitative description given earlier, thermal fluctuations of a body around an equilibrium temperature T imply random fluctuations of current, which constitutes the source term of thermal radiation. In Ampère's law (Eq. (1b)), the current density \mathbf{J} has been combined (using Ohm's law) with the electric permittivity, leading to a complex electric permittivity ϵ . For insulator, the current density $\mathbf{J} \rightarrow 0$, and then $\epsilon \rightarrow \hat{\epsilon}$. Therefore, to account for the random thermal fluctuations of current in the Maxwell equations (which are present regardless of the nature of the materials), an extraneous current density term should be added in Ampère's law [8]:

$$\nabla \times \mathbf{H}(\mathbf{r}, \omega) = -i\omega \epsilon \mathbf{E}(\mathbf{r}, \omega) + \mathbf{J}'(\mathbf{r}, \omega) \quad (\text{Ampère's law}) \quad (3)$$

The current density \mathbf{J}' plays the role of a random external source causing thermal fluctuations of the field [8]. By using Ampère's law as given by Eq. (3), instead of Eq. (1b), the Maxwell equations

become stochastic in nature (due to the fact that \mathbf{J}^r is a random variable) and are referred as the “stochastic Maxwell equations.” This is the basis of the FE.

The problem of finding a model for emission of thermal radiation needs to be considered more thoroughly. It is still necessary to relate the strength of the fluctuations of current density \mathbf{J}^r with the local temperature of the emitting body. The link between these two quantities is made via the fluctuation-dissipation theorem (FDT). Before going through the FDT, it is necessary to obtain an explicit expression for the flux of energy rather than for the electric and magnetic fields; this is shown in the next subsection.

Solution of the stochastic Maxwell equations Many different approaches can be used to solve the Maxwell equations. In the current study, the method of potentials is adopted [14]. From Gauss’s law (Eq. (1d)) and the vector identity $\nabla \cdot (\nabla \times \mathbf{A}) = 0$, the magnetic induction \mathbf{B} can be written: $\mathbf{B}(\mathbf{r}, \omega) = \nabla \times \mathbf{A}(\mathbf{r}, \omega)$, where \mathbf{A} is referred as the magnetic vector potential. This expression is then substituted in the right-hand side of Faraday’s law (Eq. (1a)):

$$\nabla \times (\mathbf{E}(\mathbf{r}, \omega) - i\omega \mathbf{A}(\mathbf{r}, \omega)) = 0 \quad (4)$$

From the vector identity $\nabla \times (\nabla \Phi_e) = 0$ and Eq. (4), the electric field can be written as:

$$\mathbf{E}(\mathbf{r}, \omega) = i\omega \mathbf{A}(\mathbf{r}, \omega) - \nabla \Phi_e(\mathbf{r}, \omega) \quad (5)$$

where Φ_e is referred as the electric scalar potential. Ampère’s law (Eq. (3)) is then manipulated to express a relation between the magnetic vector potential and the electric scalar potential:

$$\nabla \times \nabla \times \mathbf{A}(\mathbf{r}, \omega) = \mu_0 \mathbf{J}^r(\mathbf{r}, \omega) + i\omega \varepsilon \mu_0 \nabla \Phi_e(\mathbf{r}, \omega) + \omega^2 \varepsilon \mu_0 \mathbf{A}(\mathbf{r}, \omega) \quad (6)$$

The above equation can be manipulated using the vector identity $\nabla^2 \mathbf{A} = -\nabla \times \nabla \times \mathbf{A} + \nabla \nabla \cdot \mathbf{A}$, and the fact that $k^2 = \omega^2 \varepsilon \mu_0$:

$$(\nabla^2 + k^2) \mathbf{A}(\mathbf{r}, \omega) = \nabla \nabla \cdot \mathbf{A}(\mathbf{r}, \omega) - \mu_0 \mathbf{J}^r(\mathbf{r}, \omega) - i\omega \varepsilon \mu_0 \nabla \Phi_e(\mathbf{r}, \omega) \quad (7)$$

To close the problem, the Lorentz gauge is used to establish the relation between the magnetic vector potential and electric scalar potential [14]:

$$\nabla \cdot \mathbf{A}(\mathbf{r}, \omega) = i\omega \varepsilon \mu_0 \Phi_e(\mathbf{r}, \omega) \quad (8)$$

The substitution of the Lorenz gauge in Eq. (7) leads to:

$$(\nabla^2 + k^2) \mathbf{A}(\mathbf{r}, \omega) = -\mu_0 \mathbf{J}^r(\mathbf{r}, \omega) \quad (9)$$

which is the scalar Helmholtz equation. An expression for \mathbf{A} is obtained by considering the impulse response of the system:

$$(\nabla^2 + k^2) g(\mathbf{r}, \mathbf{r}', \omega) = -\delta(|\mathbf{r} - \mathbf{r}'|) \quad (10)$$

where g is the Green’s function (known function), and \mathbf{r} and \mathbf{r}' denote a field and source point, respectively. Physically, the Green’s function is the solution of the field for a point source (described by the Dirac function in Eq. (10)). By subtracting Eq. (10), multiplied by \mathbf{A} , to Eq. (9), multiplied by g , and by applying Green’s second identity [14], it can be shown that:

$$\mathbf{A}(\mathbf{r}, \omega) = \mu_0 \int_V \mathbf{J}^r(\mathbf{r}', \omega) g(\mathbf{r}, \mathbf{r}', \omega) dV' \quad (11)$$

Physically, this equation means that the solution for the field due to a source \mathbf{J}^r is the convolution of the Green’s function with that source. The magnetic vector potential given by Eq. (11) and Lorenz gauge (Eq. (8)) are then substituted in Eq. (5) to give the following expression for the electric field observed at \mathbf{r} due to a source located at \mathbf{r}' :

$$\mathbf{E}(\mathbf{r},\omega) = i\omega\mu_0 \left[1 + \frac{1}{k^2} \nabla \nabla \cdot \right] \int_V \mathbf{J}^r(\mathbf{r}',\omega) g(\mathbf{r},\mathbf{r}',\omega) dV' \quad (12)$$

Using the relation previously derived $\mathbf{B} = \nabla \times \mathbf{A}$, the magnetic field \mathbf{H} follows directly from Eq. (11):

$$\mathbf{H}(\mathbf{r},\omega) = \int_V \nabla \times \mathbf{J}^r(\mathbf{r}',\omega) g(\mathbf{r},\mathbf{r}',\omega) dV' \quad (13)$$

The electric and magnetic fields given by Eqs. (12) and (13) are derived in terms of the Green's function for the scalar wave equation (Eq. (9)). This suggests that the Green's function of Eq. (10) is the solution of an infinitesimal electric dipole pointed in a given orthogonal direction [16]. Similar expressions for the electric and magnetic fields can be derived for sources pointed in the two other orthogonal directions. By juxtaposing the three solutions, the electric and magnetic fields can be written respectively as [14,16,17]:

$$\mathbf{E}(\mathbf{r},\omega) = i\omega\mu_0 \int_V dV' g(\mathbf{r},\mathbf{r}',\omega) \left[\bar{\bar{\mathbf{I}}} + \frac{1}{k^2} \nabla \nabla \right] \cdot \mathbf{J}^r(\mathbf{r}',\omega) \quad (14a)$$

$$\mathbf{H}(\mathbf{r},\omega) = \nabla \times \int_V dV' g(\mathbf{r},\mathbf{r}',\omega) \bar{\bar{\mathbf{I}}} \cdot \mathbf{J}^r(\mathbf{r}',\omega) \quad (14b)$$

where the dyadic $\bar{\bar{\mathbf{I}}}$ is called an idem factor [16], which is in fact a 3×3 identity matrix. In Eq. (14a), the following term is called the electric dyadic Green's function [14,16]:

$$\bar{\bar{\mathbf{G}}}^e(\mathbf{r},\mathbf{r}',\omega) = g(\mathbf{r},\mathbf{r}',\omega) \left[\bar{\bar{\mathbf{I}}} + \frac{1}{k^2} \nabla \nabla \right] \quad (15)$$

Similarly, the magnetic dyadic Green's function is given by [14,16]:

$$\bar{\bar{\mathbf{G}}}^m(\mathbf{r},\mathbf{r}',\omega) = \nabla \times (g(\mathbf{r},\mathbf{r}',\omega) \bar{\bar{\mathbf{I}}}) \quad (16)$$

and the electric and magnetic dyadic Green's functions are related by the following relation:

$$\bar{\bar{\mathbf{G}}}^m(\mathbf{r},\mathbf{r}',\omega) = \nabla \times \bar{\bar{\mathbf{G}}}^e(\mathbf{r},\mathbf{r}',\omega) \quad (17)$$

Note that the dyadic Green's functions are 3×3 matrices, and are alternatively referred as the Green's tensors. Finally, the electric and magnetic fields, written as a function of the dyadic Green's functions, are given by [16,17]:

$$\mathbf{E}(\mathbf{r},\mathbf{r}',\omega) = i\omega\mu_0 \int_V dV' \bar{\bar{\mathbf{G}}}^e(\mathbf{r},\mathbf{r}',\omega) \cdot \mathbf{J}^r(\mathbf{r}',\omega) \quad (18a)$$

$$\mathbf{H}(\mathbf{r},\mathbf{r}',\omega) = \int_V dV' \bar{\bar{\mathbf{G}}}^m(\mathbf{r},\mathbf{r}',\omega) \cdot \mathbf{J}^r(\mathbf{r}',\omega) \quad (18b)$$

Equations. (18a) and (18b) give the electric and magnetic fields observed in a medium of volume V due to a current density vector \mathbf{J}^r located at \mathbf{r}' in a source medium of volume V' .

In heat transfer calculations, one is interested in calculating the radiative heat flux exchanged by the bodies instead of the electric and magnetic fields. The Poynting vector gives the instantaneous energy flux carried by a wave as a function of the electric and magnetic fields. However, no devices can measure this instantaneous energy flux. The time-averaged Poynting vector, which can be measured, is expressed as [2,18]:

$$\begin{aligned}\langle \mathbf{S}(\mathbf{r}, \omega) \rangle &= 4 \times \frac{1}{2} \text{Re} \left\{ \langle \mathbf{E}(\mathbf{r}, \omega) \times \mathbf{H}^*(\mathbf{r}, \omega) \rangle \right\} \\ &= 2 \text{Re} \left\{ \hat{\mathbf{x}}(E_y H_z^* - E_z H_y^*) + \hat{\mathbf{y}}(E_z H_x^* - E_x H_z^*) + \hat{\mathbf{z}}(E_x H_y^* - E_y H_x^*) \right\}\end{aligned}\quad (19)$$

Note that an extra factor 4 is included in the definition of the Poynting vector, since only positive frequencies are considered in the Fourier decomposition of the time-dependent fields into frequency-dependent quantities [18]. Also, the following convention is used to represent a scalar component of the fields (both electric or magnetic):

$$\begin{aligned}E_x &= i\omega\mu_0 \int_V dV' (G_{xx}^e \hat{\mathbf{x}} + G_{xy}^e \hat{\mathbf{y}} + G_{xz}^e \hat{\mathbf{z}}) \cdot (J_x^r \hat{\mathbf{x}} + J_y^r \hat{\mathbf{y}} + J_z^r \hat{\mathbf{z}}) \\ &= i\omega\mu_0 \int_V dV' (G_{xx}^e J_x^r + G_{xy}^e J_y^r + G_{xz}^e J_z^r) = i\omega\mu_0 \int_V dV' G_{xn}^e J_n^r\end{aligned}\quad (20)$$

where the subscript n involves the summation over the three orthogonal components (j is used for the magnetic field vector). By substituting the electric and magnetic components of the fields into Eq. (19), a general relation for the Poynting vector (radiative heat flux) is found:

$$\langle \mathbf{S}(\mathbf{r}, \omega) \rangle = 2 \text{Re} \left\{ i\omega\mu_0 \int_V dV' \int_V dV'' \begin{bmatrix} \hat{\mathbf{x}}(G_{yn}^e G_{zj}^{m*} - G_{zn}^e G_{yj}^{m*}) \\ + \hat{\mathbf{y}}(G_{zn}^e G_{xj}^{m*} - G_{xn}^e G_{zj}^{m*}) \\ + \hat{\mathbf{z}}(G_{xn}^e G_{yj}^{m*} - G_{yn}^e G_{xj}^{m*}) \end{bmatrix} \langle J_n^r(\mathbf{r}', \omega) J_j^{r*}(\mathbf{r}'', \omega) \rangle \right\}\quad (21)$$

Here the only unknown is the quantity $\langle J_n^r(\mathbf{r}', \omega) J_j^{r*}(\mathbf{r}'', \omega) \rangle$, which act as a source term of thermal radiation. This variable is stochastic in nature, and should be correlated to the local temperature of the medium since the randomness of the current density is due to the thermal fluctuations; this is discussed next.

The fluctuation-dissipation theorem In expressing the Poynting vector, the spectral density of the current density is needed (see Eq. (21)). The bridge between the spectral density of the fluctuating current sources and the local temperature of a body is provided by the fluctuation-dissipation theorem (FDT). It is subjected to the following assumptions: (i) the bodies are in local thermodynamic equilibrium, and an equilibrium temperature T , around which there are fluctuations, can be defined; (ii) the media are isotropic; (iii) the media are non-magnetic and are defined by a frequency-dependent dielectric constant $\varepsilon_r(\omega)$; (iv) the dielectric constant is local in space (i.e., the polarization at a given point in a medium is directly proportional to the electric field at that point, and does not directly depends on the fields from other points [17]), and consequently the fluctuations are uncorrelated between neighboring volume elements [17,18]. In general, the FDT is not limited to electrodynamics. It was applied to thermal radiation for the first time by Rytov [19]. A simple and intuitive derivation of this theorem is provided in [20,21], which is summarized below.

The FDT can be seen as a general relationship between the microscopic fluctuations of a linear dissipative body in thermal equilibrium to its macroscopic parameters (resistance and temperature). A generalized force F can be related to a generalized velocity \dot{V} via the impedance Z as:

$$F(\omega) = Z(\omega) \dot{V}(\omega)\quad (22)$$

The FDT states that at thermodynamic equilibrium, the spectral density of the generalized force is given by [20]:

$$\langle F^2(\omega) \rangle = \frac{\hbar\omega}{2\pi} \text{Re}\{Z(\omega)\} \coth\left(\frac{\hbar\omega}{2k_B T}\right) = \hbar\omega \left[\frac{1}{2} + \frac{1}{\exp(\hbar\omega/k_B T) - 1} \right] \frac{\text{Re}\{Z(\omega)\}}{\pi} \quad (23)$$

In the above, the zero point energy $\hbar\omega/2$ can be neglected. Indeed, in calculating the radiative flux, this term drops out due to the fact that it is always compensated by the surrounding of the body [8]. Equation (23) can therefore be re-written as:

$$\langle F^2(\omega) \rangle = \frac{\text{Re}\{Z(\omega)\} \Theta(\omega, T)}{\pi} \quad (24)$$

where $\Theta(\omega, T)$ is the mean energy of a Planck oscillator in thermal equilibrium at an angular frequency ω and at temperature T . From the vector-wave equation [21], the following relation between the current density and electric field can be obtained:

$$\mathbf{J}^r(\mathbf{r}, \omega) = \left[\frac{-1}{\Delta V'} \left(\frac{i}{\omega\mu_0} \nabla \times \nabla \times + \omega\varepsilon_0 (\text{Im}\{\varepsilon_r(\omega)\} - i \text{Re}\{\varepsilon_r(\omega)\}) \right) \right] \mathbf{E}(\mathbf{r}, \omega) \Delta V' \quad (25)$$

If we compare Eq. (25) with Eq. (22), we see that the generalized force is the current density \mathbf{J}^r , the term inside brackets is the impedance, and the product $\mathbf{E} \Delta V'$ represents a generalized velocity. By applying the general FDT (Eq. (24)), the spectral density of the current fluctuations is given by:

$$\langle J_n^r(\mathbf{r}', \omega) J_j^{r*}(\mathbf{r}'', \omega) \rangle = \frac{\omega\varepsilon_0}{\pi} \text{Im}\{\varepsilon_r(\omega)\} \Theta(\omega, T) \delta_{nj} \delta(\mathbf{r}' - \mathbf{r}'') \quad (26)$$

where the Dirac function is present due to the locality of the dielectric constant (i.e., the fluctuations are correlated in the limit $\mathbf{r}'' \rightarrow \mathbf{r}'$), while the Kronecker function accounts for the assumption of isotropic media. It can also be seen that Eq. (26) only involves the imaginary part of the dielectric constant which describes the absorption/dissipation of thermal radiation inside an irradiated body.

The spectral density of the fluctuating currents (Eq. (26)) can then be substituted in the Poynting vector (radiative heat flux) given by Eq. (21):

$$\langle \mathbf{S}(\mathbf{r}, \omega) \rangle = \frac{2\varepsilon_0\mu_0\omega^2}{\pi} \text{Re} \left\{ i \int_V dV' \int_V dV'' \begin{bmatrix} \hat{\mathbf{x}}(G_{yn}^e G_{zj}^{m*} - G_{zn}^e G_{yj}^{m*}) \\ + \hat{\mathbf{y}}(G_{zn}^e G_{xj}^{m*} - G_{xn}^e G_{zj}^{m*}) \\ + \hat{\mathbf{z}}(G_{xn}^e G_{yj}^{m*} - G_{yn}^e G_{xj}^{m*}) \end{bmatrix} \text{Im}\{\varepsilon_r(\omega)\} \Theta(\omega, T) \delta_{nj} \delta(\mathbf{r}' - \mathbf{r}'') \right\} \quad (27)$$

Equation (27) is a general relation for the radiative heat flux which accounts for the near-field effects of thermal radiation since it has been derived from the Maxwell equations. For a given geometry and boundary conditions, the components of the dyadic Green's functions must be calculated [16,17,22,23]. Results of near-field versus far-field radiative heat transfer are presented next.

RESULTS

The problem of radiant energy exchange between two semi-infinite layers spaced by a vacuum gap of thickness d is considered. The variations of the radiative flux heat flux are with respect to the z -axis (normal to the layers), and the x -axis is collinear with the surfaces of the plates. The two layers are labeled media 1 and 2, while the vacuum is referred as medium 0. The net total radiative heat flux between media 1 and 2 is found by substitution of the appropriate components of the dyadic Green's function for 1D layered media [16,22]; after several mathematical manipulations, this leads to the following expressions [12,24]:

$$q_{1-2}^{net,prop} = \pi\omega_0^2 \int_{\omega=0}^{\infty} [I_{b,\omega}(T_1) - I_{b,\omega}(T_2)] \frac{d\omega}{\omega^2} \times \int_{k_x=0}^{\omega/c_0} \left[\frac{(1-|r_{01}^s|^2)(1-|r_{02}^s|^2)}{|1-r_{01}^s r_{02}^s \exp(2ik'_{z,0}d)|^2} + \frac{(1-|r_{01}^p|^2)(1-|r_{02}^p|^2)}{|1-r_{01}^p r_{02}^p \exp(2ik'_{z,0}d)|^2} \right] k_x dk_x \quad (28a)$$

$$q_{1-2}^{net,evan} = 4\pi\omega_0^2 \int_{\omega=0}^{\infty} [I_{b,\omega}(T_1) - I_{b,\omega}(T_2)] \frac{d\omega}{\omega^2} \int_{k_x=\omega/c_0}^{\infty} \exp(-2k''_{z,0}d) \times \left[\frac{\text{Im}\{r_{01}^s\}\text{Im}\{r_{02}^s\}}{|1-r_{01}^s r_{02}^s \exp(-2k''_{z,0}d)|^2} + \frac{\text{Im}\{r_{01}^p\}\text{Im}\{r_{02}^p\}}{|1-r_{01}^p r_{02}^p \exp(-2k''_{z,0}d)|^2} \right] k_x dk_x \quad (28b)$$

Equation (28a) is the net total radiative heat flux due to propagating modes, while Eq. (28b) is due to evanescent modes. The propagating modes are those calculated in the geometric optics approach, while the evanescent modes are usually not accounted for. The evanescent modes propagate along the surfaces of media 1 and 2, but decay exponentially in the z -direction over a distance less than a wavelength. If medium 1 is emitting in the free space, the net energy flux from the evanescent field is consequently zero. If medium 2 is brought close enough to medium 1 such that its surface lies in the evanescent field, the motion of the charges in medium 2 are affected by the presence of this near-field. The resulting electronic motion dissipates the energy of the near-field in medium 2 by Joule heating; then, a net radiative transfer due to the evanescent modes occurs between media 1 and 2. This phenomenon is called radiation tunneling, and can be seen as an extra channel in which the radiant energy can flow, causing the radiative transfer between bodies to exceed the values predicted by the Planck blackbody distribution. The distinction between the propagating and evanescent modes is reflected by the integration over the x -component of the wavevector (k_x) in Eqs. (28). The z -component of the wavevector in the vacuum $k_{z,0}$ is given by $(k_0^2 - k_x^2)^{1/2}$, where k_0 is the magnitude of the wavevector in the vacuum ($= \omega/c_0$). Here, k_x is a pure real number due to invariance in the x -direction, and since ω is always real and positive, k_0 is also real and positive. Given that, $k_{z,0}$ is a pure real number for $0 \leq k_x \leq \omega/c_0$ (propagating modes), and a pure imaginary number when $k_x > \omega/c_0$ (evanescent modes). Propagating wave interferences are accounted for in Eq. (28a) via the term $\exp(2ik'_{z,0}d)$. It can be shown that Eq. (28a), in the far-field limit, reduces to the radiative flux obtained from the geometric optics approach [12,24]. The evanescent contribution (Eq. (28b)) vanishes at this limit, due to the exponentially decaying term.

The integral terms of Eqs. (28) are solved numerically using Simpson's method. For the integration over k_x from ω/c_0 to infinity, a relative difference of 0.1 % between consecutive steps is used for convergence [24]. The limit of integration for the angular frequencies can easily be found for a far-field radiative transfer problem (by calculating the proportion of energy emitted in a given spectral region [9,10]). Due to radiation tunneling in the near-field, these spectral limits should be extended over a broader range [24]. For the calculation of total fluxes, an iterative procedure is adapted and a relative difference of 0.1% between the iterations is considered as convergence criterion. The code, implemented in *Fortran*, has been validated for dielectric materials [21] and for materials involving surface phonon-polaritons [25]. The overall computational uncertainty is found to be less than 2%.

For the first set of simulation, both media are assumed to be dielectric materials, with the same frequency-independent dielectric constant of $\epsilon_r = 20 + i0.0001$; their respective temperatures are taken as $T_1 = 800$ K and $T_2 = 200$ K. The dominant wavelengths of thermal radiation, as predicted by Wien's law, are approximately 3.6 and 14.5 μm for temperatures of 800 and 200 K, respectively. We should consequently expect dominant near-field effects for gap thicknesses below these approximate thresholds. The net monochromatic radiative heat flux is reported in Fig. 1(a), for

different gap thicknesses d , as a function of the angular frequency ω ; the relative contributions of propagating and evanescent modes on the total (i.e., integrated over all angular frequencies) radiative flux are shown in Fig. 1(b) as a function of d .

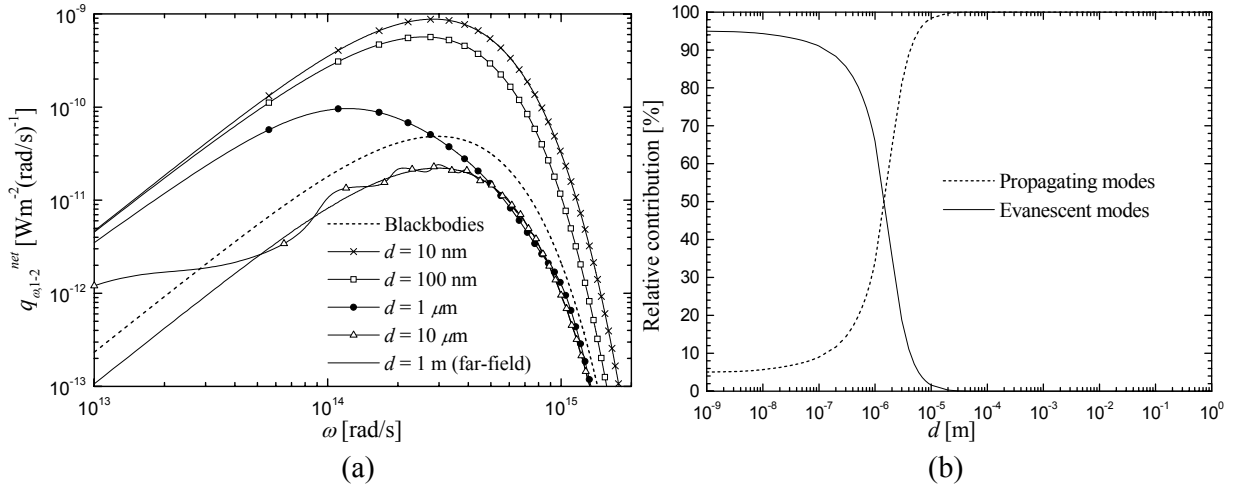


Figure 1. Radiative heat transfer between two semi-infinite layers, at $T = 800$ K and 200 K, spaced by a vacuum. (a) Net monochromatic radiative heat flux as a function of the angular frequency. (b) Relative contribution from propagating and evanescent modes as a function of the gap thickness.

As seen in Fig. 1(a), the monochromatic radiative heat flux increases as d decreases. The radiative heat flux between two blackbodies is also shown in Fig. 1(a) to illustrate the fact that values obtained in the near-field can exceed the Planck distribution by few orders of magnitude. For dielectric materials, the maximum radiative transfer in the limit $d \rightarrow 0$ is given by $n^4/(n^2+n'^2)$ times the blackbody radiation ($n^2 = \epsilon_r$) [21,26]. Obviously, and as expected, in the far-field limit the radiative heat flux becomes independent of d . The large values of the radiative heat flux obtained at smaller gap distances, for 10 nm, 100 nm, and $1 \mu\text{m}$, are due to the tunneling of evanescent waves. As the gap thickness decreases, a more important proportion of evanescent waves are tunneled leading to an increase of the radiative heat flux. This is confirmed by Fig. 1(b), where it is shown that for 10 nm, 100 nm, and $1 \mu\text{m}$, approximately 95%, 93%, and 65% of the radiative flux is due to evanescent modes, respectively. For $10 \mu\text{m}$, the tunneling of evanescent waves is almost negligible (contribution of approximately 2%), while the interference phenomenon becomes dominant, which can be seen in Fig. 1(a) by the oscillatory behavior of the radiative heat flux.

Near-field radiative heat transfer problems have been solved in the case of two parallel plates [3,12,21,23-25], for 1D multi-layered media [21,25,27], for 2D cylindrical regions [28], between a half-space and a small sphere (dipolar approximation) [23,29,30], and between two large spheres [31], to name only few of them. Also, if polar or metallic materials are considered, the radiative heat transfer can take place in a very narrow range of frequency due to the resonant excitation of surface polaritons (phonons and plasmons). Discussion on this subject can be found in references [2,12,18,21,23,25,28].

Despite all these works, there is still an important unanswered question: at which length scale the classical theory of radiation fails to describe correctly a radiation heat transfer problem? In other words, at what length scale near-field effects should be taken into account? Of course, the criterion based on Wien's law provides an approximate length scale. However, as research continues at the nanoscale, this question becomes less academic and carries more practical importance to define a strict length scale for which the near-field effects have to be taken into account. Our work is currently examining that subject, and we show our preliminary results for the geometry discussed above.

In the following simulations, medium 2 is modeled as a heat sink ($T_2 = 0$ K). Results are plotted, as a function of the product dT_1 , in terms of the normalized net total radiative heat flux, which is the sum of Eqs. (28a) and (28b) divided by the net total radiative flux in the far-field. Note that this far-field flux has been calculated independently from the equation obtained using a ray tracing method. The influence of T_1 (for a fixed ϵ_r) is shown in Fig. 2(a), while the influence of the real part of the dielectric constant ϵ_r' (for a fixed T_1) is presented in Fig. 2(b).

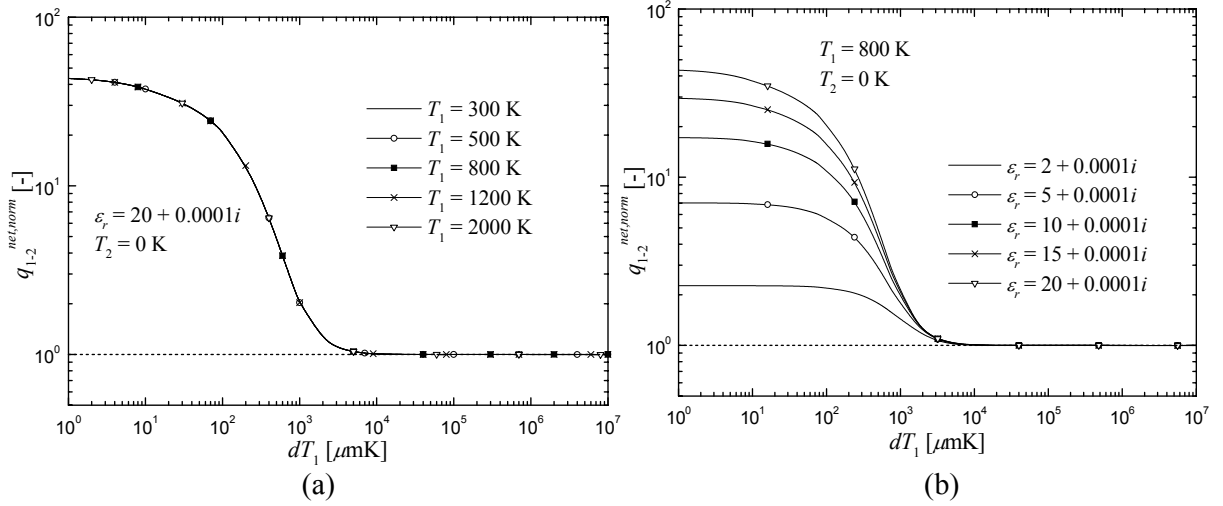


Figure 2. Normalized net total radiative heat flux as a function of dT_1 . (a) Influence of the temperature T_1 . (b) Influence of the real part of the dielectric constant ϵ_r' .

It can be seen in Fig. 2(a) that when the normalized radiative flux is plotted against the variable dT_1 , all curves overlap, regardless of T_1 . The relative differences between the values of $q_{1-2}^{net, norm}$ (for the five different T_1 considered) for each dT_1 vary from 7.7×10^{-8} to 0.64 %, which fall in the computational uncertainty range. Figure 2(b) shows that the normalized radiative flux increases as ϵ_r' increases (Fig. 2(b)). On the other hand, the normalized fluxes seem to converge toward the same values of dT_1 as $q_{1-2}^{net, norm} \rightarrow 1$.

The far-field regime is reached when the normalized radiative flux is 1. However, in the simulations, the normalized radiative flux never reaches the exact value of 1; starting from dT_1 of approximately $6 \times 10^4 \mu\text{mK}$, the normalized flux oscillates around 1 (maximum of $\pm 0.25\%$). This can be explained by the fact that for large values of d , the integrand of Eqs. (28a) is highly oscillatory [24]. It becomes therefore impossible to predict the exact length scale for transition from the near- to the far-field regime using these numerical simulations. On the other hand, we can define approximate criteria for which 90%, 95%, and 99% of the radiative flux is due to the far-field regime (i.e., the criteria are based on the inverse of the normalized radiative fluxes). Moreover, results of Fig. 2 suggest that these length scales are function of only two variables, namely dT_1 and the dielectric constant ϵ_r .

From the data obtained to plot Fig. 2(a), 90%, 95%, and 99% of the radiative flux is due to the far-field regime for dT_1 of 2977 μmK , 4443 μmK , and 9056 μmK , respectively. Despite the fact that these length scales are subjected to numerical errors when performing the integration, it shows clearly that the transition from the near- to the far-field regime is above the length scale given by Wien's law (2898 μmK). If we consider a temperature T_1 of 800 K, the length scales based on the 90%, 95%, and 99% are 3.72 μm , 5.55 μm , and 11.32 μm , while the criterion based on Wien's law gives 3.62 μm . Therefore, the criterion based on Wien's law gives a good order of magnitude for the length scale, assuming that approximately 10% of the radiative flux is due to near-field effects.

The same criteria are applied to the data of Fig. 2(b). The length scales based on the 90, 95, and 99% criteria are respectively: (i) 2513, 3645, and 7032 μmK (for $\varepsilon_r' = 2$); (ii) 2911, 4033, and 7827 μmK (for $\varepsilon_r' = 5$); (iii) 3014, 4306, and 8483 μmK (for $\varepsilon_r' = 10$); (iv) 3029, 4402, and 8832 μmK (for $\varepsilon_r' = 15$); (v) 3030, 4437, and 9053 μmK (for $\varepsilon_r' = 20$). These results suggest that as the real part of the dielectric constant increases, near-field effects have influence for larger values of dT_1 . For example, the relative increase of dT_1 between the case $\varepsilon_r' = 2$ and 20, for the criterion 90%, is 18.7 %. Note also that dT_1 for $\varepsilon_r' = 20$ found using the data from Fig. 1(a) are not exactly the same than those obtained from the data of Fig. 2(b). This is explained by the fact that the values of dT_1 have been found in Fig. 2(a) using the average of the five temperatures, while the dT_1 have been calculated from Fig. 2(b) using the data at 800 K. The maximum relative difference between these two set of calculations is 1.75%, which falls in the computational uncertainty range.

The results of this section have suggested that the criterion for transition from near- to far-field radiative transfer based on Wien's law may be acceptable, with the disclaimer that approximately 10% of the radiative flux will still be due to near-field effects. On the other hand, it is important to note that the length scale at which $q_{1-2}^{net, norm} \rightarrow 1$ (based on the 99% criterion) is about three times larger than Wien's law. The analysis will be extended for lossy dielectric materials, systems involving two half-space of different dielectric constants, and to materials that can support surface polaritons (metals and polar crystals).

SUMMARY

Radiative heat transfer can be considered within two distinct regimes. The first is given by the classical theory of radiation, based on geometric optics/ray tracing, in which the radiative transfer equation (RTE) is used; this is the far-field regime. The second is the near-field regime in which the Maxwell equations must be solved. It should be understood that the electromagnetic wave approach can be used unilaterally at all length scales and requires the solution of the Maxwell equations with proper boundary conditions. However, the computational requirements are usually prohibitive once the computational domain reaches to a span of a few wavelengths. The RTE is used to overcome this difficulty and to bring a clear understanding to practical problems.

Acknowledgements MF is grateful to the Natural Sciences and Engineering Research Council of Canada (NSERC) for their financial support (ES D3 scholarship). Additional funding for this work is received from the College of Engineering, University of Kentucky.

REFERENCES

1. Wong, B.T. and Mengüç, M.P., Electronic Thermal Conduction in Thin Gold Films, *ASME Summer Heat Transfer Conference*, Las Vegas, July 21-23, 2003, HT2003-47172.
2. Chen, G., *Nanoscale Energy Transport and Conversion*, Oxford University Press, New York, New York, 2005.
3. Polder, D. and Van Hove, M., Theory of Radiative Heat Transfer between Closely Spaced Bodies, *Physical Review B*, Vol. 4, No. 10, pp 3303-3314, 1971.
4. Cravalho, E.G., Tien, C.L. and Caren, R.P., Effect of Small Spacings on Radiative Transfer between Two Dielectrics, *ASME Journal of Heat Transfer*, Vol. 89C, pp 351-358, 1967.
5. Boehm, R.F. and Tien, C.L., Small Spacing Analysis of Radiative Transfer between Parallel Metallic Surfaces, *ASME Journal of Heat Transfer*, Vol. 92C, No. 3, pp 405-411, 1970.
6. Mishchenko, M.I., Maxwell's Equations, Radiative Transfer, and Coherent Backscattering: A General Perspective, *Journal of Quantitative Spectroscopy and Radiative Transfer*, Vol. 101, pp. 540-555, 2006.
7. Mishchenko, M.I., Travis, L.D. and Lacis, A.A., *Multiple Scattering of Light by Particles: Radiative Transfer and Coherent Backscattering*, Cambridge University Press, Cambridge, 2006.

8. Rytov, S.M., Kravtsov, Y.A. and Tatarskii, V.I., *Principles of Statistical Radiophysics 3: Elements of Random Fields*, Springer-Verlag Berlin Heidelberg, New York, 1983.
9. Siegel, R. and Howell, J., *Thermal Radiation Heat Transfer*, 4th edition, Taylor & Francis, New York, New York, 2002.
10. Modest, M.F., *Radiative Heat Transfer*, 2nd edition, Academic Press, San Diego, California, 2003.
11. Kidd, R., Ardini, J. and Anton, A., Evolution of the Modern Photon, *American Journal of Physics*, Vol. 57, No. 1, pp. 27-35, 1989.
12. Mulet, J.-P., Joulain, K., Carminati, R. and Greffet, J.-J., Enhanced Radiative Heat Transfer at Nanometric Distances, *Microscale Thermophysical Engineering*, Vol. 6, pp 209-222, 2002.
13. Whale, M.D., A Fluctuational Electrodynamics Analysis of Microscale Radiative Heat Transfer and the Design of Microscale Thermophotovoltaic Devices, *Ph.D. Thesis*, MIT, Cambridge, 1997.
14. Peterson, A.F., Ray, S.L. and Mittra, R., *Computational Methods for Electromagnetics*, Oxford University Press, New York, New York, 1998.
15. Jackson, J.D., *Classical Electrodynamics*, 3rd edition, Academic Press, New York, 1998.
16. Tai, C.-T., *Dyadic Green Functions in Electromagnetic Theory*, 2nd edition, IEEE Press, New York, New York, 1994.
17. Tsang, L., Kong, J.A. and Ding, K.H., *Scattering of Electromagnetic Waves*, Wiley, New York, New York, 2000.
18. Mulet, J.-P., Modélisation du Rayonnement Thermique par une Approche Électromagnétique. Rôle des Ondes de Surfaces dans le Transfert d'Énergie aux Courtes Échelles et dans les Forces de Casimir, *Ph.D. Thesis*, Université Paris-Sud 11, Paris, 2003.
19. Rytov, S.M., Correlation Theory of Thermal Fluctuations in an Isotropic Medium, *Soviet Physics JETP*, Vol. 6, No. 1, pp 130-140, 1958.
20. Landau, L.D. and Lifshitz, E.M., *Electrodynamics of Continuous Media*, Addison-Wesley, Reading, Massachusetts, 1960.
21. Narayanaswamy, A. and Chen, G., Direct Computation of Thermal Emission from Nanostructures, *Annual Review of Heat Transfer*, Vol. 14, pp 169-195, 2005.
22. Sipe, J.E., New Green-Function Formalism for Surface Optics, *Journal of Optical Society of America B*, Vol. 4, No. 4, pp 481-489, 1987.
23. Joulain, K., Mulet, J.-P., Marquier, F., Carminati, R. and Greffet, J.-J., Surface Electromagnetic Waves Thermally Excited: Radiative Heat Transfer, Coherence Properties and Casimir Forces Revisited in the Near Field, *Surface Science Reports*, Vol. 57, pp 59-112, 2005.
24. Fu, C.J. and Zhang, Z.M., Nanoscale Radiation Heat Transfer for Silicon at Different Doping Levels, *International Journal of Heat and Mass Transfer*, Vol. 49, No. 4, pp 1703-1718, 2006.
25. Narayanaswamy, A. and Chen, G., Surface Modes for Near Field Thermophotovoltaics, *Applied Physics Letters*, Vol. 82, No. 20, pp 3544-3546, 2003.
26. Pan, J.L., Choy, H.K.H. and Fonstad Jr, C.G., Very Large Radiative Transfer over Small Distances from a Black Body for Thermophotovoltaic Applications, *IEEE Transactions on Electron Devices*, Vol. 47, No. 1, pp 241-249, 2000.
27. Narayanaswamy, A. and Chen, G., Thermal Radiation in 1D Photonic Crystals, *Journal of Quantitative Spectroscopy and Radiative Transfer*, Vol. 93, pp 175-183, 2005.
28. Hammonds Jr., J.S., Thermal Transport via Surface Phonon Polaritons Across a Two-Dimensional Pore, *Applied Physics Letters*, Vol. 88, 041912, 2006.
29. Mulet, J.P., Joulain, K., Carminati, R. and Greffet, J.-J., Nanoscale Radiative Heat Transfer between a Small Particle and a Plane Surface, *Applied Physics Letters*, Vol. 78, No. 19, pp 2931-2933, 2001.
30. Pendry, J.B., Radiative Exchange of Heat between Nanostructures, *Journal of Physics: Condensed Matter*, Vol. 11, pp 6621-6633, 1999.
31. Narayanaswamy, A. and Chen, G., Near-Field Radiative Energy Transfer between Two Spheres, *Proceedings of IMECE2006*, Chicago, November 5-10, 2006, IMECE2006-15845.